Acta Crystallographica Section D
Biological Crystallography
ISSN 0907-4449

A neutron diffraction study of purple membranes under pressure

Isabelle Gundel Rossand,[a] Giuseppe Zaccai[a,b]* and Giovanna Fragneto[b]

[a]Institut de Biologie Structurale, Grenoble, France, and [b]Institut Laue–Langevin, BP 156, 38042 Grenoble, France

Correspondence e-mail: zaccai@ill.fr

Received 16 May 2010
Accepted 21 September 2010

Neutron diffraction from hydrated stacks of natural two-dimensional crystal patches of purple membrane from *Halobacterium salinarum* was studied as a function of pressure. Measurements in H_2O and D_2O permitted the determination of the distribution of water of hydration in the in-plane projection of the membrane. The main experimental difference observed between the samples at 300 MPa and atmospheric pressure was a major reorganization of the hydration around the lipid head groups and protein, associated with a protein conformational change and small reductions in lamellar (stacking) and in-plane lattice spacings, which was consistent with the compressibility of membrane-protein and lipid components.

1. Introduction

Purple membranes (PMs) are structured patches in the plasma membrane of the extreme halophilic archaeon *Halobacterium salinarum*. The colour of PMs arises from the integral membrane retinal-binding protein bacteriorhodopsin (BR; 75% of the PM mass), which is organized with specific lipids (25% of the PM mass). BR functions as a light-activated proton pump that generates a proton gradient across the membrane; the absorption of one photon by retinal results in the transfer of one proton from the cytoplasmic side to the extracellular side of the membrane. A millisecond time-scale photocycle of retinal absorption maxima is associated with the proton-pumping activity (Oesterhelt, 1998; Haupts *et al.*, 1999). The structure of BR in the natural membrane was solved to a few angstroms resolution by electron microscopy on single membrane samples, revealing its organization in seven transmembrane α-helices, which became paradigmatic of an important family of membrane proteins (Grigorieff *et al.*, 1996). Neutron diffraction using hydrogen/deuterium labelling of PM stacks contributed significantly to describing the location of retinal, the organization of hydration and the specific lipids in the natural membrane (Jubb *et al.*, 1984; Zaccai & Gilmore, 1979; Rogan & Zaccai, 1981; Papadopoulos *et al.*, 1990; Weik *et al.*, 1998; Zaccai, 2000). After obtaining highly ordered BR microcrystals from cubic lipid phases (reviewed by Chiu *et al.*, 2000), the structure of the protein was solved to high resolution by X-ray crystallography and was studied by various groups in order to propose molecular mechanisms for the proton-pump activity (Pebay-Peyroula *et al.*, 1997; Essen *et al.*, 1998; Belrhali *et al.*, 1999; Luecke *et al.*, 1999; Lanyi & Schobert, 2003; Yamamoto *et al.*, 2009). The role of hydration and temperature on the BR photocycle has been studied in

order to characterize the thermodynamics of the proton pump (Varo & Lanyi, 1991*a*,*b*). In PM films equilibrated at a relative humidity (rh) of between 80 and 100% the photocycle takes place in a characteristic time similar to that of PM in aqueous suspension. Proton activity is slowed below 80% rh and ceases at 60% rh. Neutron diffraction has been used to determine the localization of hydration water in the membrane as a function of rh. At high humidity the hydration level around the lipid polar head groups is predominant, while at reduced humidity the water molecules withdraw from the lipids and it is possible to count the number of water molecules in the proton channel (Zaccai & Gilmore, 1979; Rogan & Zaccai, 1981; Papadopoulos *et al.*, 1990). A neutron diffraction study with H_2O/D_2O exchange revealed that not only does the lamellar (stacking) parameter decrease at lower rh owing to a smaller water layer between membranes, but the parameter of the in-plane hexagonal PM lattice also decreases because of dehydration around the lipid head groups (Zaccai, 1987); in the same paper it was shown that the hexagonal PM in-plane lattice parameter also decreases (by about 2%) at 77 K with respect to room temperature. However, the H_2O/D_2O-exchange experiments clearly showed that the contraction, while similar to that arising from low rh, does not arise from a 'freeze-drying' type of dehydration; the hydration structure is maintained intact at low temperature, suggesting that the decrease in unit-cell parameter is a consequence of the thermal contraction of all membrane components. A hypothesis that inhibition of PM activity arises from 'stiffer' molecular dynamics at low rh and low temperature (Zaccai, 1987) was subsequently supported by direct measurements of membrane dynamics as a function of temperature and rh by neutron spectroscopy, which also revealed a dynamical transition in PM similar to previous observations in soluble proteins (Ferrand *et al.*, 1993; Lehnert *et al.*, 1998).

PM remains the best-characterized natural membrane with respect to structure and dynamics and a highly tractable model to study their relation to biological function and activity. The key to success in such studies is the parallel dependence on hydration, temperature and pressure of structure and dynamics on one hand and of activity, as reflected by the photocycle kinetics, on the other. Pressure is a thermodynamic parameter that provides important complementary information to temperature. High-pressure macromolecular crystallography has been actively developed to provide an efficient tool for the high-resolution exploration of functional conformers and intermediates (Fourme *et al.*, 2009). The effects of pressure on the structure and dynamics of PM have not yet been fully explored. Varo & Lanyi (1995) examined the photocycle under hydrostatic pressure up to 100 MPa and interpreted the activation-volume changes in terms of BR conformation and hydration changes. Klink *et al.* (2002) extended the pressure to 400 MPa and took measurements at 298 and 313 K to develop a model that explained the dependence of the activation-volume change in the transition to the longer-lived photocycle intermediate (the M state) by the electrostriction effect of the charges that are formed and neutralized during the transition. The interest of studying the effects of pressure on the structure of PM is that it becomes possible to separate the volume changes arising from compression from contraction arising from thermal energy. Pressure can induce phase transitions (for example, protein denaturation at room temperature) and even lead to unknown phases at room temperature. High-pressure studies are also of physiological relevance and have biotechnological applications. Barophilic organisms live at depths of 10 000 m in deep ocean trenches and experience pressures of up to 100 MPa. Even though such pressures influence the structure and therefore the function of biological membranes, there are prokaryotic species that have adapted to these extreme conditions. Mesophilic organisms that are not adaptable to these conditions change their morphology and stop reproducing at 40–50 MPa. The biotechnological applications of pressure have been reviewed by Heremans & Smeller (1998). In 1895, H. Royer used high pressure to kill bacteria. In 1899 Bert Hite examined the effects of pressure on milk, meat, fruits and vegetables, and in 1914 Bridgman measured the physical and thermal properties of water and various solutions under pressure and coagulated egg albumen under high pressure. The first commercial pressure-processed food products were introduced in Japan in 1990. Since the year 2000 a wide variety of pressure-treated products have also become available commercially in the USA and Europe, ranging from processed food to vaccines and pharmaceuticals.

Here, we present neutron diffraction results on the effects on the structure and hydration of PM in stacked multilamellar samples. We determined the lamellar and in-plane lattice parameters, the in-plane projection of the BR structure and the hydration distribution (by H_2O/D_2O exchange) as a function of pressure up to 300 MPa. Despite the fact that BR activity ceases at about 100 MPa pressure, the diffraction data revealed that the two-dimensional crystal structure of PM is maintained at 300 MPa, with a significant redistribution of membrane hydration and a conformational change in BR involving helix-tilt movements, which we discuss in terms of volume-reducing protein–water and protein–lipid head group interactions.

2. Materials and methods

H. salinarum cultures were prepared according to the protocol of Oesterhelt & Krippahl (1983) and PMs were extracted and purified as described by Oesterhelt & Stoeckenius (1974). For neutron diffraction measurements, 300 µl of the purified membranes in aqueous solution (optical density 40, corresponding to a dry membrane mass of 50 mg) was deposited on a quartz slide (35 × 75 × 0.3 mm). The samples were dried in air at room temperature and rh for 4 d before mounting them in a sealed compressor chamber in the presence of a saturated salt-solution bath to control the rh. Since the quartz slides could only resist pressures of up to 300 MPa, no measurements were performed above this value. All measurements were performed at 293 K at two rh values [84% (saturated KCl) and 75% (saturated NaCl)].

Measurements were performed on the small momentum-transfer diffractometer D16 at the Institut Laue–Langevin

(http://www.ill.eu/instruments-support/instruments-groups/instruments/d16/). The measurement of the lamellar spacing was performed with the slides parallel to the incoming beam and the in-plane diffraction was measured with the sample plane perpendicular to the incoming beam. After sample alignment, both scan sets were performed using θ–2θ scans.

Lamellar reflection angular positions were used to calculate the lamellar spacings. Two-dimensional lattice structure-factor moduli, $|F(h, k)|$, were calculated from the integrated intensities of in-plane reflections normalized by the total number of incident neutrons after background subtraction and correction by the Lorentz factor. Two-dimensional Fourier maps were then calculated for each condition (hydration, pressure, H_2O/D_2O composition) from the structure factors by dividing the powder reflections into their respective (h, k) contributions and applying phases according to the electron-microscopy structure of PM, as described, for example, in Weik *et al.* (1998), Zaccai & Gilmore (1979) and Papadopoulos *et al.* (1990). Powder intensities were measured to a resolution of about 7 Å. Most peaks were well separated. The intensities $I(h, k)$ in the few which were partially overlapped were split according to peak height. Intensities with the same $h^2 + hk + k^2$ value were split according to the ratio obtained in electron diffraction. Structure factors were derived after normalization and multiplication by the Lorentz factor. They were given the corresponding phases using electron microscopy. The use of electron microscopy was justified because at this resolution the phasing is determined by the protein *versus* lipid contrast. The zero contour in the difference Fourier map corresponds to the average scattering-length density in the unit cell.

3. Results and discussion

Fig. 1 shows the evolution with time of the lamellar spacing, d, of a BR sample hydrated with a saturated KCl solution (86% rh) while varying the pressure from atmospheric to 300 MPa and back to atmospheric. The initial increase in lamellar spacing arises from the swelling of the membrane during the hydration process. At 100 MPa, the d-spacing decreases very rapidly and continues decreasing until the maximum pressure of 300 MPa. Upon decreasing the pressure the d-spacing increases again. After correcting for hydration equilibration, a reduction in d-spacing of 0.8 Å is calculated at 300 MPa with respect to atmospheric pressure. This is a small value, suggesting that the interlamellar water layer stays in place at the higher pressure, and can be accounted for by the compressibility of the various membrane components.

The variation of the in-plane lattice parameter a as a function of time while increasing the pressure to 300 MPa and decreasing it again to atmospheric pressure is plotted in Fig. 2. The lattice spacing decreases when pressure is applied and increases reversibly when the pressure is decreased. Fig. 3 shows the effect at the two rh values studied (75 and 86%); in both cases the reduction in the a value is about 1.3 Å. A

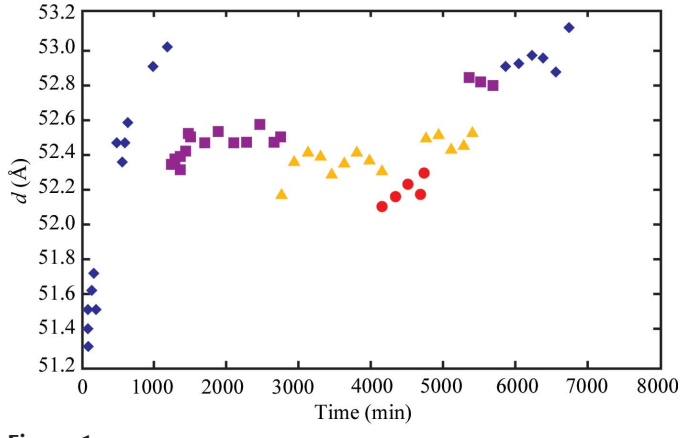

Figure 1
Diagram of the lamellar spacing, d, of purple membrane stacks as a function of time measured at 293 K and a relative humidity of 86% (from a saturated KCl solution) at the following pressures: atmospheric (diamonds), 100 MPa (squares), 200 MPa (triangles) and 300 MPa (circles).

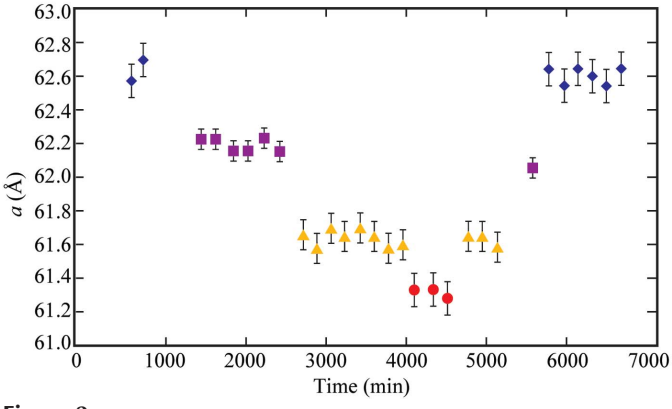

Figure 2
Diagram of the lattice-spacing value, a, of purple membrane stacks as a function of time measured at 293 K and a relative humidity of 86% (from a saturated KCl solution) at the following pressures: atmospheric (diamonds), 100 MPa (squares), 200 MPa (triangles) and 300 MPa (circles).

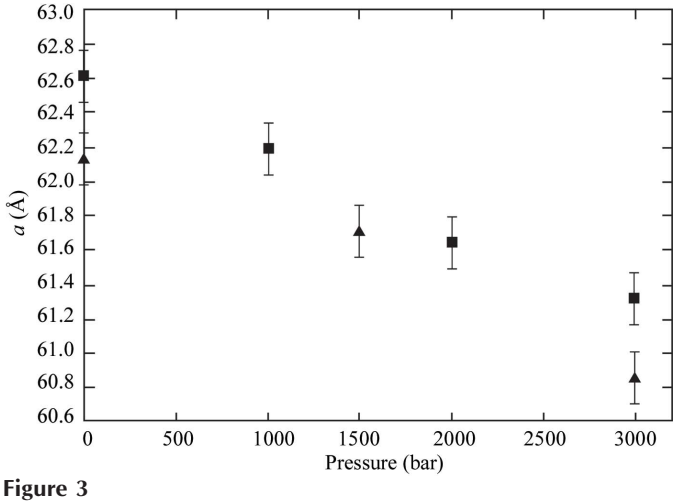

Figure 3
Diagram of the lattice spacing value, a, of purple membrane stacks as a function of applied pressure at a relative humidity of 75% (triangles) from saturated NaCl solution and 86% (squares) from saturated KCl solution.

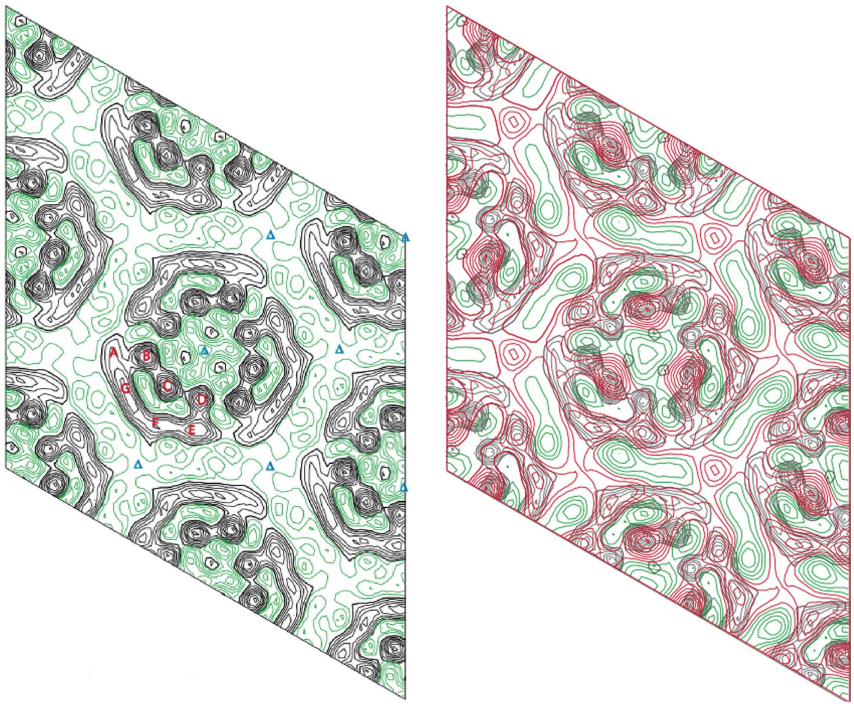

(*a*) (*b*)

Figure 4
(*a*) Two-dimensional Fourier map of PM in H_2O (75% rh) at 300 MPa pressure. Positive contours in black correspond to the BR helix projections as identified by the letters A–G. Negative contours denoting the lipid projections are shown in green. (*b*) Difference Fourier map between PM (H_2O, 75% rh) at atmospheric pressure and at 300 MPa. The lattice parameter was chosen to be 61.5 Å for this plot; this corresponds to the mean of the lattice parameters at the two pressures. Positive and negative contours are shown in red and green, respectively. As a guide to the eye, the BR projection under the same rh conditions at atmospheric pressure is shown in grey.

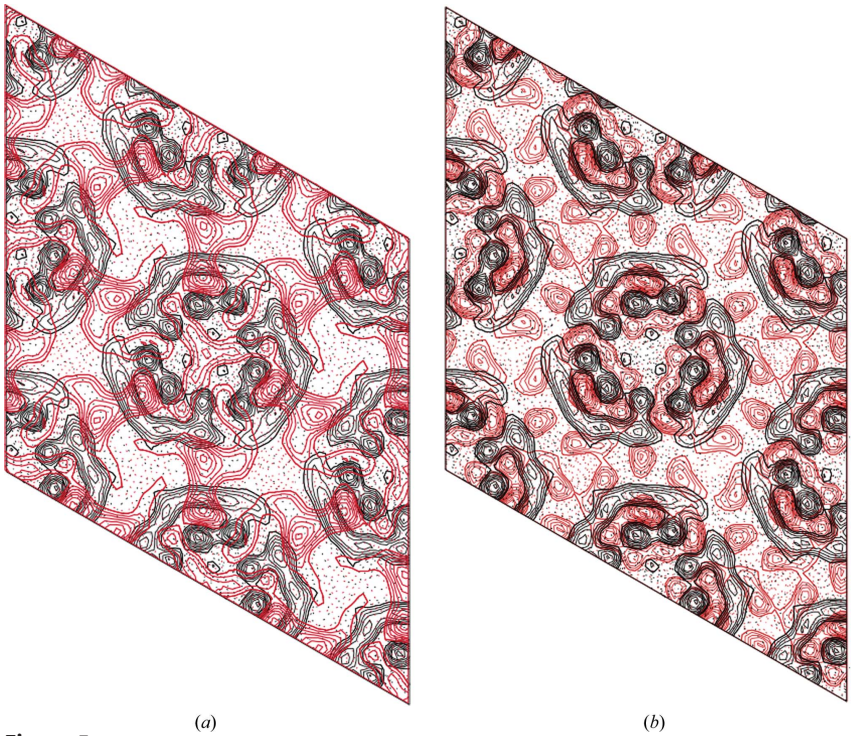

(*a*) (*b*)

Figure 5
(*a*) Hydration pattern of PM obtained from D_2O/ H_2O difference Fourier maps at 75% rh and atmospheric pressure. (*b*) Hydration pattern of PM obtained from D_2O/ H_2O difference Fourier maps at 75% rh and 300 MPa.

similar reduction in the in-plane lattice parameter has previously been observed upon dehydration or cooling of the membrane (Zaccai, 1987); the Fourier maps of the difference conditions were therefore examined in order to determine the structural and hydration changes associated with the high-pressure reduction of the lattice parameter.

The two-dimensional Fourier map of PM in H_2O (75% rh) at 300 MPa pressure is shown in Fig. 4(*a*). Clearly, the membrane maintains its well known two-dimensional organization at high pressure; the positive contours in black correspond to the BR helix projections as identified by the letters A–G. Negative contours denoting the lipid projections are shown in green. The difference Fourier map between PM (H_2O, 75% rh) at atmospheric pressure and at 300 MPa, however, indicated a small structural rearrangement (Fig. 4*b*). In plotting the difference map, the lattice parameter was chosen to be 61.5 Å (the mean of the lattice parameters at the two pressures). Positive and negative contours are shown in red and green, respectively. As a guide to the eye, the BR projection under the same rh conditions at atmospheric pressure is shown in grey. The difference density contour levels (red or green) represent 10% of the grey contour levels. The main feature of the difference map is a positive peak on the C side of helix B with negative peaks on either side, suggesting a small clockwise rotation of the pair of helices at high pressure. The statistical r.m.s. contributes to less than one contour.

The hydration patterns of PM obtained from D_2O/H_2O difference Fourier maps (at 75% rh) are shown in Fig. 5(*a*) (atmospheric pressure) and Fig. 5(*b*) (300 MPa). The proton-channel hydration peak inside BR between helices B and G dominates the 75% rh map at atmospheric pressure. Polar-head hydration peaks are also observed in the lipid areas of the map. D_2O/H_2O difference maps have been placed on an absolute scattering-density scale by calibrating them against features of known scattering density in order to 'count' the water molecules in the features (Zaccai & Gilmore, 1979; Papadopoulos *et al.*, 1990). The features in Fig. 5(*a*) correspond closely to the water molecules expected in the proton channel and around the lipid head groups. Significant differences are observed at high pressure (Fig. 5*b*). The hydration peaks inside the protein projection are more intense, with a corresponding decrease in lipid

area peaks (recall that the difference map zero contour level corresponds to the average difference density in the unit cell, so that the maps only show fluctuations around the average). A prominent peak also appears at high pressure in the pockets between helices A and B and D and E of adjacent symmetry-related BR molecules. Since it is not known whether the water content of the membrane changes with pressure, two interpretations are possible: (i) dehydration of the membrane caused by the pressure and (ii) the movement of water molecules within the membrane. As referred to above, dehydration of the membrane induces a reduction of the in-plane lattice parameter by a similar value to that observed with pressure. On the other hand, on dehydration a much larger reduction than the observed 0.8 Å would be expected for the lamellar spacing. Reductions in the *d*-spacing of a few angstroms corresponding to at least one layer of water have been observed upon lowering the rh. Note also the increase in lamellar spacing upon hydration equilibration at the start of the measurements shown in Fig. 1. Furthermore, it is known from previous work on similar PM samples (see also Fig. 1) that the equilibration of membrane hydration and dehydration is very slow (on a time scale of hours), while the pressure effect on the structural parameters was practically immediate (Figs. 1 and 2*a*). These considerations tend to exclude an interpretation in terms of pressure-induced dehydration. As discussed above, the linear changes in the *d*-spacing and two-dimensional lattice parameter with pressure can be interpreted as arising from volume changes (compression) in the membrane components without dehydration. The hydration differences that are observed in the Fourier map would then be a consequence of a rearrangement of water in the membrane projection induced by pressure. The data revealed that under pressure water molecules moved from around the lipid head groups towards protein groups within the pocket formed by the helices, the long negatively charged carboxy-terminal loop and the A–B and D–E bridge regions between neighbouring symmetry-related BR molecules (Fig. 5*b*). Water interactions with ions, polar and apolar groups are extremely complex and depend on various factors, including the group charge, size, steric geometry and hydrogen-bonding capability, as well as on the water dipole geometry and hydrogen bonding (Fedorov *et al.*, 2007). These observations suggest that water interactions with protein groups in PM are favoured by pressure because they lead to a smaller volume than hydration around lipid head groups. This is understandable in terms of waters and counterions such as Na^+, for example, that interact with large anions such as the phosphate groups in the lipid head groups occupying a larger volume than when they interact with protein carboxyl groups.

4. Conclusions

Four effects of 300 MPa pressure on PM at 293 K hydrated to 75% and 86% rh were observed: (i) a reduction in the lamellar spacing of 0.8 Å, (ii) a reduction in the two-dimensional lattice spacing of about 1.3 Å, (iii) a conformational rearrangement around helices B and C and (iv) a major reorganization of membrane hydration, with water moving from the lipid head-group areas to the protein. Various volume-reduction factors will influence the behaviour of the membrane under pressure and lead to these observations. The main factors are the compressibility of the main components of the membrane (protein, lipids and water) and the volume changes in the different ion–water interactions with protein and lipid groups.

The authors are happy to acknowledge the ILL for beamtime, the high-pressure laboratory for support and Bruno Demé for help during the measurements. We are very grateful to Professor Dieter Oesterhelt, Dr Frank Gabel and Dr Martin Weik for scientific discussions and assistance with PM preparation.

References

Belrhali, H., Nollert, P., Royant, A., Menzel, C., Rosenbusch, J. P., Landau, E. M. & Pebay-Peyroula, E. (1999). *Structure*, **7**, 909–917.
Chiu, M. L., Nollert, P., Loewen, M. C., Belrhali, H., Pebay-Peyroula, E., Rosenbusch, J. P. & Landau, E. M. (2000). *Acta Cryst.* D**56**, 781–784.
Essen, L., Siegert, R., Lehmann, W. D. & Oesterhelt, D. (1998). *Proc. Natl Acad. Sci. USA*, **95**, 11673–11678.
Fedorov, M. V., Goodman, J. M. & Schumm, S. (2007). *Phys. Chem. Chem. Phys.* **9**, 5423–5435.
Ferrand, M., Dianoux, A. J., Petry, W. & Zaccai, G. (1993). *Proc. Natl Acad. Sci. USA*, **90**, 9668–9672.
Fourme, R., Girard, E., Kahn, R., Dhaussy, A. C. & Ascone, I. (2009). *Annu. Rev. Biophys.* **38**, 153–171.
Grigorieff, N., Ceska, T. A., Downing, K. H., Baldwin, J. M. & Henderson, R. (1996). *J. Mol. Biol.* **259**, 393–421.
Haupts, U., Tittor, J. & Oesterhelt, D. (1999). *Annu. Rev. Biophys. Biomol. Struct.* **28**, 367–399.
Heremans, K. & Smeller, L. (1998). *Biochim. Biophys. Acta*, **1386**, 353–370.
Jubb, J. S., Worcester, D. L., Crespi, H. L. & Zaccai, G. (1984). *EMBO J.* **3**, 1455–1461.
Klink, B. U., Winter, R., Engelhard, M. & Chizhov, I. (2002). *Biophys. J.* **83**, 3490–3498.
Lanyi, J. K. & Schobert, B. (2003). *J. Mol. Biol.* **328**, 439–450.
Lehnert, U., Reat, V., Weik, M., Zaccai, G. & Pfister, C. (1998). *Biophys. J.* **75**, 1945–1952.
Luecke, H., Schobert, B., Richter, H. T., Cartailler, J. P. & Lanyi, J. K. (1999). *J. Mol. Biol.* **291**, 899–911.
Oesterhelt, D. (1998). *Curr. Opin. Struct. Biol.* **8**, 489–500.
Oesterhelt, D. & Krippahl, G. (1983). *Ann. Microbiol. (Paris)*, **134**B, 137–150.
Oesterhelt, D. & Stoeckenius, W. (1974). *Methods Enzymol.* **31**, 667–678.
Papadopoulos, G., Dencher, N. A., Zaccai, G. & Buldt, G. (1990). *J. Mol. Biol.* **214**, 15–19.
Pebay-Peyroula, E., Rummel, G., Rosenbusch, J. P. & Landau, E. M. (1997). *Science*, **277**, 1676–1681.
Rogan, P. K. & Zaccai, G. (1981). *J. Mol. Biol.* **145**, 281–284.
Varo, G. & Lanyi, J. K. (1991*a*). *Biochemistry*, **30**, 5016–5022.
Varo, G. & Lanyi, J. K. (1991*b*). *Biophys. J.* **59**, 313–322.
Varo, G. & Lanyi, J. K. (1995). *Biochemistry*, **34**, 12161–12169.
Weik, M., Patzelt, H., Zaccai, G. & Oesterhelt, D. (1998). *Mol. Cell*, **1**, 411–419.
Yamamoto, M., Hayakawa, N., Murakami, M. & Kouyama, T. (2009). *J. Mol. Biol.* **393**, 559–573.
Zaccai, G. (1987). *J. Mol. Biol.* **194**, 569–572.
Zaccai, G. (2000). *Biophys. Chem.* **86**, 249–257.
Zaccai, G. & Gilmore, D. J. (1979). *J. Mol. Biol.* **132**, 181–191.